Journal of Fundamental and Applied Sciences

Research Article

ISSN 1112-9867

Available online at http://www.jfas.info

LINEAR ANNULAR ANTENNAS ARRAY DESIGN BY EVOLUTIONARY ALGORITHMS: A COMPARATIVE STUDY

Hichem Chaker[1], Abri Mehadji[2], Hadjira Badaoui[3]

[1]RCAM Laboratory, Department of electronics, Faculty of electrical engineering, University Djillali Liabes, Sidi Bel Abbès, Algeria

[2]Department of Telecom, Faculty of Technology, University Abou Bekr Belkaid, Tlemcen, Algeria

[3]Department of Telecom, Faculty of Technology, University Abou Bekr Belkaid, Tlemcen, Algeria

Received: 18 March 2021 / Accepted: 20 April 2022 / Published online: 21 April 2022

ABSTRACT

This paper exposes a comparative study that was made between the adaptive particle swarm optimization (APSO) and the hybrid model genetical swarm optimizer approaches (GSO) for the synthesis of 1-D equally spaced annular ring antenna arrays for both TM_{11} and TM_{12} modes. The synthesis of 1-D uniform antenna arrays is designed as a mono-objective problem. The employed optimization techniques are compared in terms of convergence rate and side lobes level reduction. Several original numerical results are provided to demonstrate the performance of the proposed techniques. The results reveal that the suggested array antenna synthesis approach using genetical swarm optimizer outperforms the adaptive particle swarm optimization in terms of side lobes level reduction and convergence rate.

Keywords: Ring microstrip antenna; Linear Antenna Arrays; Genetical swarm optimization GSO; Adaptive particle swarm optimization APSO; TM_{11} and TM_{12} modes.

Author Correspondence, e-mail: mh_chaker2005@yahoo.fr

doi: http://dx.doi.org/10.4314/jfas.1118

1. INTRODUCTION

The microstrip antennas arrays find utilization in high-accomplishment spacecrafts, aircrafts, mobile applications, satellites and missiles, where cost, weight, size, achievement, flexibility, and miniature antennas are required. Currently, there are several commercial applications, such as radar, wireless communication and mobile radio that have similar requirements where this sort of printed antennas can be exploited [1-2]. The literature about printed antennas arrays [3-5] exposes a wide range of methods of synthesis. The array pattern synthesis problem can be defined as that of finding the array excitations to produce the required antenna radiation patterns [6-7]. Schultz and Bergman (1955) studied the structure of the annular-ring. In [8], the author noted that this kind of micro strip antenna finds its application in the medical field as a resonator. In [9], there is a detailed survey of this structure where the author concludes that the annular ring antenna may also be broadband when operated near the TM_{12} resonance. For TM_{1m} modes, [10] have shown that this antenna is an excellent resonator when m is an odd number and a good radiator if m is an even number.

In the recent past, synthesis of microstrip antenna arrays received a great attention from researchers. A first algorithm genetic approach towards the synthesis of ring printed antenna arrays can be traced in the work of Abri [11], the algorithm genetic was applied to reduce the side lobes peaks. Ibarra in [12] applied the differential evolution to design of concentric ring antenna arrays for isoflux radiation considers the optimization of the spacing between rings and the amplitude excitation across the antenna elements. In [13] Panduro applied the non-dominated sorting genetic algorithm to design of non-uniform circular phased arrays. In [14], the author uses the linear programming method in the design of antenna patterns with prescribed nulls and other constraints, an improved version of particle swarm optimization was used by Deng [15] to minimizing sidelobe levels and facilitating null placements of nonlinear antenna arrays. In [16] another version of particle swarm optimization method called unified particle swarm optimization with random ternary variables was presented and applied to antenna array synthesis, the design of conformal antennas arrays is optimized using immunity tactic is given in [17]. Recently RAVI [18] applied the differential evolution algorithm for the synthesis of phased array antenna for side lobe level reduction.

In the present contribution, we present results concerning the synthesis and optimization of uniform linear printed annular-ring microstrip antennas arrays through the use of the adaptive particle swarm optimization and the hybrid model genetical swarm optimizer for two TM_{11} and TM_{12} modes. A comparative evaluation of the two approaches in the performance to design 1-D annular-ring antennas arrays will be provided. The simulation results show the success of the applied algorithms of synthesis.

In terms of organization, the paper is structured, besides the introduction, in four sections. Section 2 portrays the global radiation patterns of linear arrays. Overviews of adaptive particle swarm optimization and genetical swarm optimizer are described in section 3. The comparative study is dealt with in section 4. Finally, conclusions are given in section 5.

2. PROBLEM FORMULATION

The far radiated field ring antenna in a point M is situated in the plane $(\vec{u}_\theta, \vec{u}_\varphi)$. The radiated field can be calculated using the Huygens's field equivalence principle as applied to the well-known field distribution at the cavity magnetic wall which is formed by the ground plane and the patch conductor. Figure 1, sketched below, shows the employed annular ring.

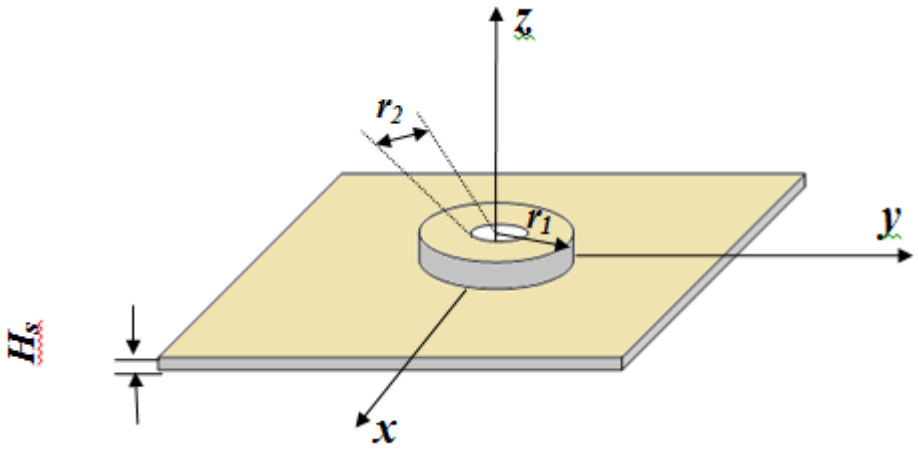

Fig.1. Ring microstrip antenna geometry

A consideration of a 1-D linear antennas array with *N* identical sources of directivity pattern $f(\theta,\varphi)$ is shown in Figure 2 in which each element is located at the position x_i. For the ring antenna directivity pattern calculation, it was opted for the dynamic permittivity model

detailed in [19-20]. Its global radiation diagram in linear arrangement is given by:

$$F_{1D}(\theta) = \sum_{i=1}^{N} f(\theta)\, a_i \cos[kx_i \cos(\theta) + \phi_i] \quad (1)$$

The elements amplitudes a_i and phases $Ø_i$ are related by the complex excitation weight $w_i = a_i e^{-jØi}$, with θ as the angular direction and k as the wave number.

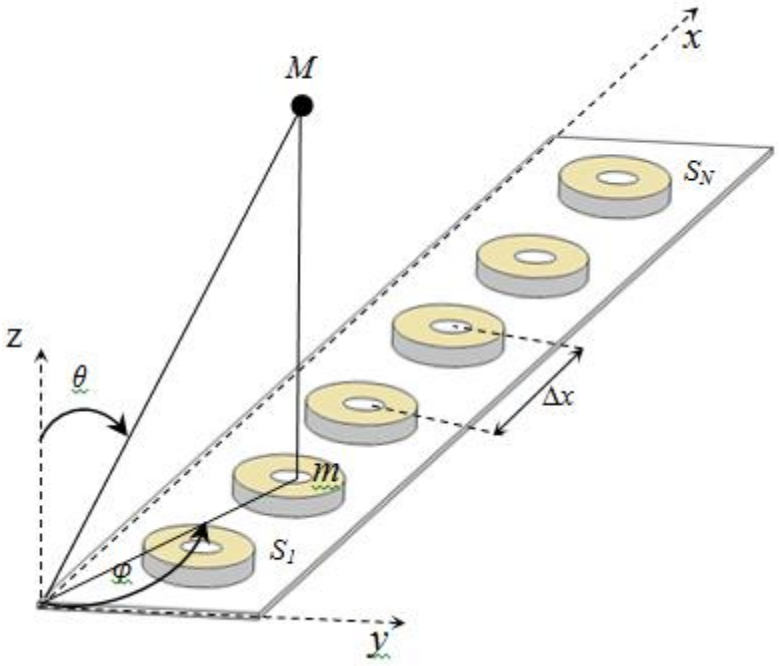

Fig.2. Linear ring antennas array.

The directivity $F(\theta,\varphi)$ is a function of the two angles of direction θ and φ. If φ is determinate, the pattern $F(\theta,\varphi)$ can be conformed in the E or H plane. In this study, interest is in the synthesis of linear arrays in the $\varphi=0$ plane.

The synthesis procedure can be achieved by minimizing a criterion of variation δ between the synthesized pattern $F_s(\theta,\varphi)$ and the desired one $F_d(\theta)$ defined by a gauge. The corresponding constrained optimization problem is defined as:

$$\delta(\theta,\varphi) = \left| F_s(\theta,\varphi) - F_d(\theta) \right| \quad (2)$$

These results were obtained from the application of a ring antennas array designed for TM_{11} and TM_{12} modes at the resonance frequencies of 2.6 GHz and 0.6 GHz, respectively. The antenna characteristics are as follows: ε_r =2.32; H_s= 1.59*mm*; r_1=35*mm*; r_2= 70*mm*. The array step Δx is fixed to 0.5Lambda.

3. ADAPTIVE PARTICLE SWARM ALGORITHM AND GENETICAL SWARM OPTIMIZER

The adaptive particle swarm optimization algorithm is considered as practical tools for synthesis of antennas arrays. Such a kind of evolutionary computational methods is inspired by the social behavior of swarms [21]. Like other evolutionary algorithms, the PSO algorithm is initialized with a population of random solutions. Each particle moves in the dimensional problem space with a velocity adjusted according to the flying experiences of its own and its neighborhood. The position of the i^{th} particle is depicted as $X_i= (x_{i1},\ldots,x_{id},\ldots,x_{iD})$. The best previous location of the i^{th} particle is saved and expressed as $P_i= (p_{i1},\ldots,p_{id},\ldots,p_{iD})$, which is named p_{best}. The symbol g denotes the index of the best p_{best} among all the particles; the location P_g is also called *gbest*. The vector $V_i= (v_{i1},\ldots,v_{id},\ldots,v_{iD})$ represents the velocity for the i^{th} particle, V_i must be in the range [$-V_{max}V_{max}$] [22].

The following Algorithm shows the process for implementing the PSO.

- Initiate a generation of particles with random positions and velocities values on *D*-dimensions in the search space.
- loop
- Calculate the desired optimization fitness function for each particle.
- Compare particle's fitness evaluation with its p_{besti}. If the present value is better than p_{besti}, then set p_{besti} equal to the current value, and p_i equal to the current location x_i.
- Identify the particle in the neighbors with the best achievement so far, and attribute its index to the variable *g*.
- changes the velocity and location toward its p_{best} and g_{best} according to the following equations:

$$V_{id}=w\times V_{id}+C_1\times rand()\times(p_{id}-x_{id})+C_2\times rand()\times(p_{gd}-x_{id}) \quad (3)$$

$$x_{id}=x_{id}+V_{id} \quad (4)$$

- If a stop criterion is satisfied (good fitness or a maximum number of generations), then exit loop.
- end loop

w is the inertia weight, C_1 and C_2 are the weighting coefficients acceleration, and *rand()* is a random function in the range [0 1] [23]. The adaptive PSO is executed by inserting the pseudo code of APSO that is shown in figure 3 in the standard PSO process.

```
int[ ]similar Count = new int[m]; // at initializa tion stage

// in standard PSO process

For (i = 0; i < m; i++) {                    // for each particle
    IF (i ≠ g && |ΔF_i| < ε)
      THEN similar Count[i]++;               // add 1
    ELSE similar Count[i] = 0;               // reset
    IF (similar Count[i] > T_c)              // predefined count
      THEN replace (the i^th particle);
    ELSE execute (step d) in standard PSO
}
```

Fig.3. Inserted pseudo code of adaptive PSO

F_i is the fitness evaluation of the i^{th} particle, F_{gbest} is the fitness of g_{best}. $\Delta F_i = f(F_i, F_{gbest})$ is an error function. The ε is a predefined constant according to the demanded precision. T_c is the count constant. The replace () function is employed to replace the i^{th} stagnant particle. ε is set as 10^{-4}, and T_c is set as 3. A swarm of 40 particles were used. C_1 and C_2 were fixed to 0.5. The upper limit of the inertia weight is 0.9, and the lower limit is 0.4. In this section, we combine two well-known global optimization methodologies: adaptive particle swarm optimization [21] and genetic algorithm [24-25]. Both approaches start with a random population of solutions, genetical swarm optimizer seems to be a good algorithm as it combines the searching abilities of both methods [6]. The Flow chart of the genetical swarm optimizer algorithm is depicted in figure 4.

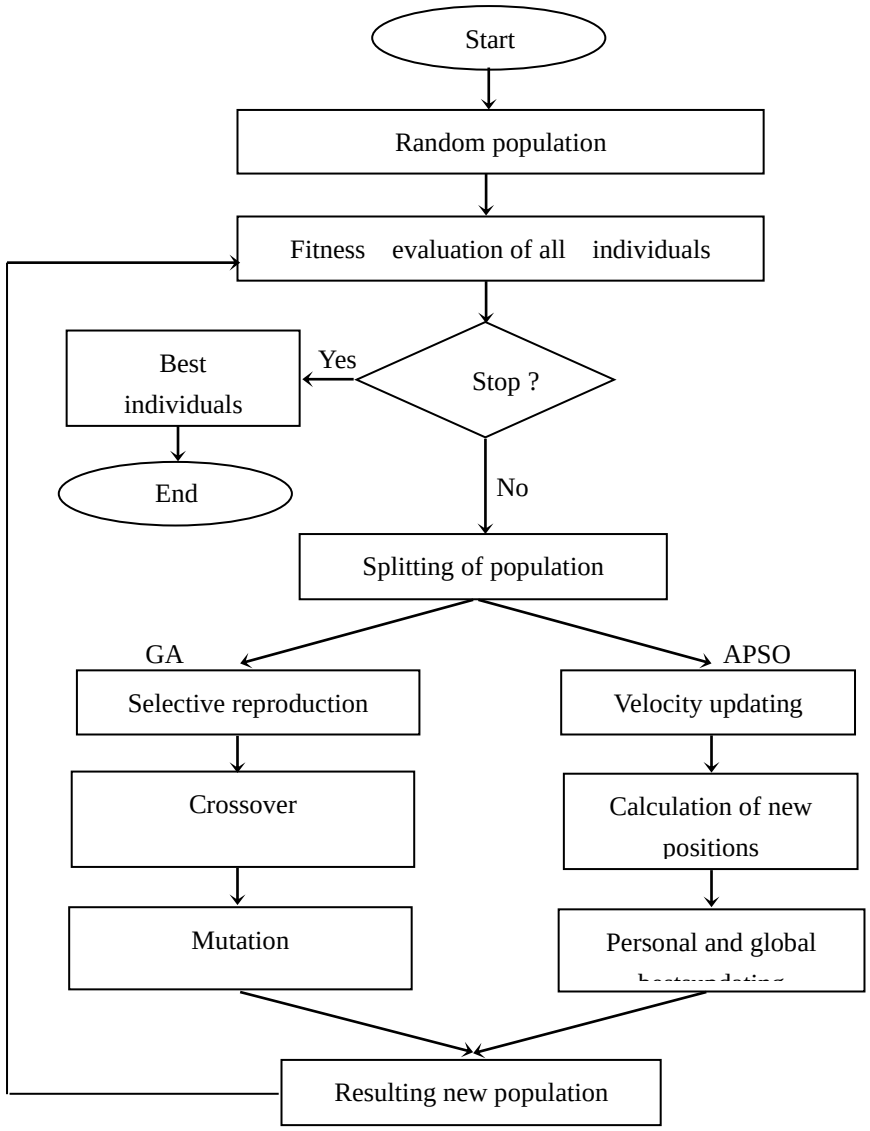

Fig.4. Flow-chart of the GSO algorithm

The hybrid model fundamentally consists of a robust collaboration of the two prominent evolutionary algorithms APSO and GA, since it preserves the integration of the two methods for the complete run procedure. In each generation, the population is split randomly into two sub-generations according to the hybridization coefficient, and they progress with the two approaches respectively. Hence, they are incorporated in the renew population which is in its turn divided into two parts in the next generation for another run of adaptive particle swarm or genetic operators. In our case, the hybridization coefficient is set to 0.5. This translates that the percentage of population evolved with APSO algorithm is equal to 50%, whereas the rest with GA technique.

4. RESULTS AND DISCUSSION

In this section, APSO and GSO are applied to 1-D antenna arrays design. For design specifications, the objective is to accomplish low side lobes level for the modes TM_{11} and $TM_{12,}$ respectively. To demonstrate the superiority of GSO, the performance of the hybrid model is compared with the APSO algorithm in each simulation. The adaptive particle swarm parameters are as follows: a number of particles equal to 40, inertia weight *w* from 0.9 to 0.4, C_1 and C_2 equal to 0.5 and T_c=3. The GSO parameters are: The population size is equal to 40, the hybridization coefficient HC= 0.5, the mutation probability P_m=0.1 and the crossover probability P_c=0.4.

We consider a 1-D array of 12 annular rings radiating elements having the same radiation pattern $f(\theta)$ [19], spaced by 0.5Lambda. In order to synthesize the array in the two modes TM_{11} and TM_{12}, the synthesis was made on 1-D array with only one parameter of optimization: the excitation amplitude of the elements. APSO is running for 90 iterations for both modes. The acceptable side lobes level should be equal to, or less than, the desired value and there are no side lobes exceeding the defined values -30 dB for fundamental mode and TM_{12} modes. Figure 5 blatantly indicates that there is a reduction in side lobes levels using GSO as compared to APSO optimized arrays. For the fundamental mode, the side lobes level of the hybrid model GSO optimized array was lowered from −30 dB to −32 dB (by about 2 dB) as compared to APSO, and from -30 dB to -35 dB (by about 5 dB) for the TM_{12} mode.

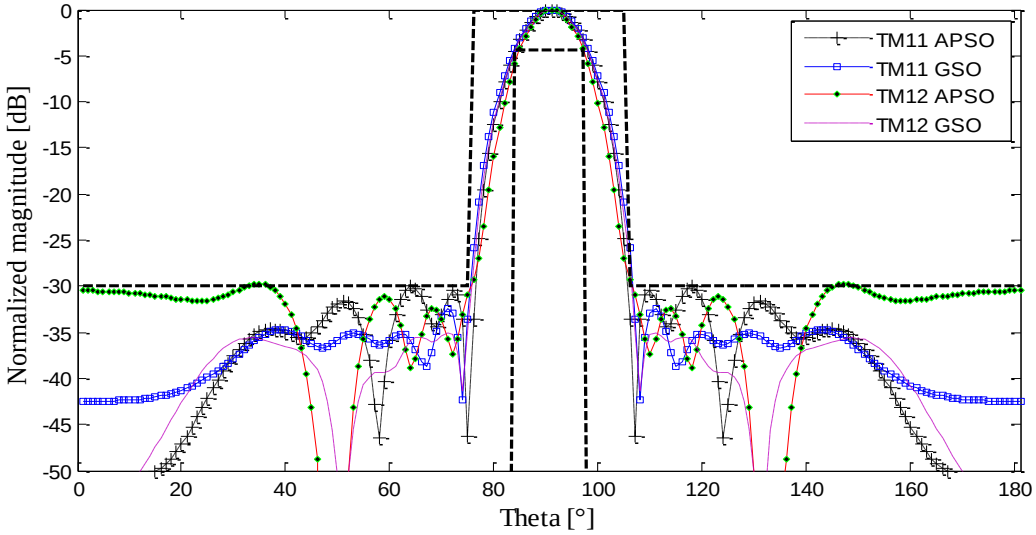

Fig.5. Radiation patterns obtained by GSO and APSO for TM_{11} and TM_{12} modes

The proposed methods have been compared in terms of the convergence speed. The minimum error values are plotted against the number of iterations to show the convergence curves of the applied techniques. It is obviously noted that the GSO outperforms the APSO in convergence speed for both modes.

It can be synthetized from figure 6 that the GSO procedure possesses the highest convergence speed CS in the optimization compared with APSO algorithm, in the case of the fundamental mode synthesis the GSO procedure converge after 64 iterations, whereas in the application of APSO algorithm the convergence is reached after 86 iterations.

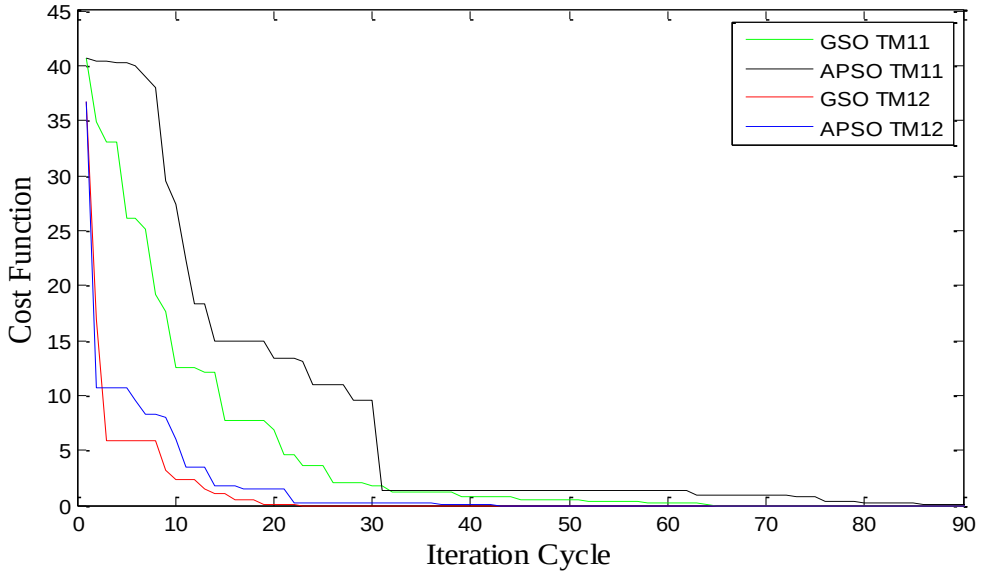

Fig.6. Comparison of GSO and APSO schemes for TM_{11} and TM_{12} modes

Numerical results for synthesizing the TM_{12} mode demonstrated the superiority of GSO over the APSO procedure. For GSO, the convergence was achieved after 19 iterations; the corresponding number of iterations is 23 for the APSO technique. In order to evaluate the performance of the hybrid model, we compare the numerical results calculated by the GSO, and the simulated annealing [20]. As such, a linear array antenna of 12 elements operated in its fundamental TM_{11} mode is regarded. We show the comparison of the far-field patterns among the GSO simulation results, and the simulated annealing results in [20]. The GSO algorithm side lobes level is -32 dB; these results remain comparable to the simulated annealing algorithm: -31.72 dB, a small improvement in the side lobes level is obtained. The excitation amplitudes of the elements are sketched in Table 1.

Table 1. Amplitudes distribution

N°	APSO TM_{11}	APSO TM_{12}	GSO TM_{11}	GSO TM_{12}
1	0.2052	0.4306	0.0513	0.0014
2	0.4525	0.6547	0.1611	0.1389
3	0.5640	0.4859	0.3243	0.3316
4	0.7979	0.9662	0.5351	0.4828
5	0.9163	0.9489	0.7246	0.6621
6	0.9757	0.9643	0.8702	0.7957
7	0.9895	0.7416	0.9408	0.7462
8	0.8210	0.7708	0.8854	0.7312
9	0.6292	0.6300	0.7894	0.7661
10	0.4184	0.2450	0.5401	0.3538
11	0.2624	0.2692	0.4075	0.2521
12	0.0768	0.2212	0.1875	0.2385

In this example, GSO and APSO are used to determine an optimal set of amplitude and phase distributions of the array composed of 14 annular elements with a distance of 0.5Lambda between the elements that generate a directive beam with minimum relative side lobes level for both modes. The results are displayed in figure 7.

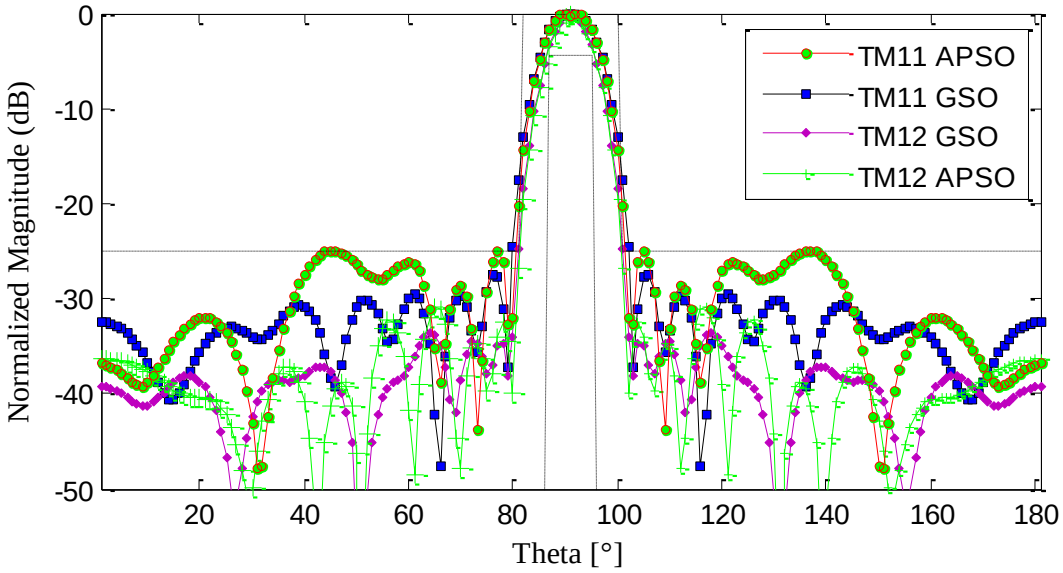

Fig.7. Radiation patterns obtained by GSO and APSO for TM_{11} and TM_{12} modes

The resulting field patterns fulfill the required restrictions, with a maximum side lobes level in the region besides the main lobe below -25 dB and -30dB in the case of APSO for TM_{11} and $TM_{12,}$ respectively. In the case of GSO, the maximum SLL is below the -27.49dB and -33.50dB for both modes, respectively. The best results of each method presented in this section are used for comparison. An improvement of 2.49 dB and 3.50dB are achieved for the TM_{11} and TM_{12} modes using GSO. It should be noted from the comparison results that the GSO not only achieves a better peak side lobes level as shown in figure 7, but it also presents a high rate of convergence compared to APSO algorithm mentioned in this paper (see figure 8). Table 2 lists the obtained amplitudes and phases distribution.

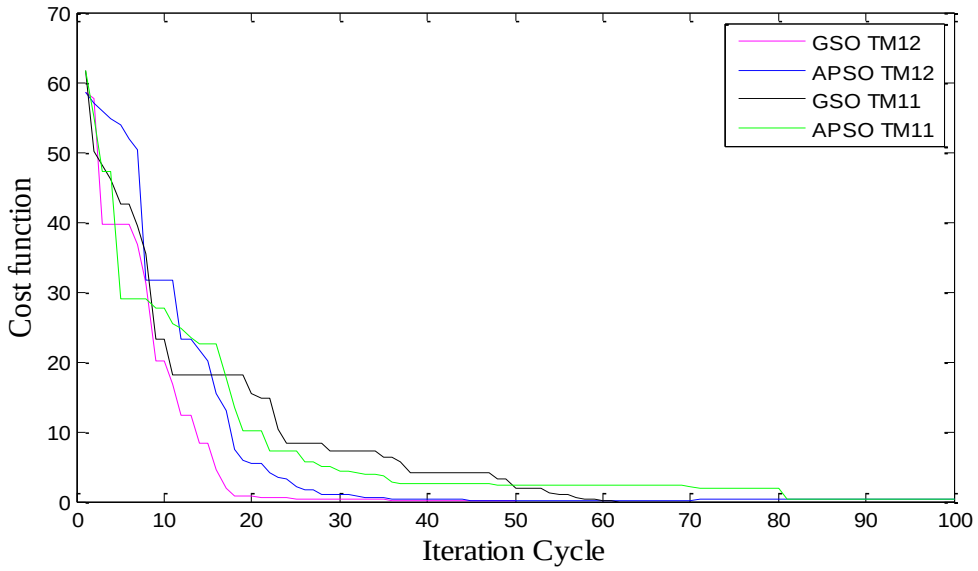

Fig.8. Comparison of GSO and APSO schemes for TM_{11} and TM_{12} modes

Table 2. Amplitudes and phases distribution

N°	APSO TM_{11}		APSO TM_{12}		GSO TM_{11}		GSO TM_{12}	
	Amplitude (V)	Phase (Rad)	Amplitude (V)	Phase (Rad)	Amplitude (V)	Phase (Rad)	Amplitude (V)	Phase (Rad)
1	0.3071	0.7823	0.3082	0.3310	0.2552	1.0129	0.3770	2.3665
2	0.8101	1.5520	0.3670	0.2695	0.6975	1.6228	0.3933	3.4577
3	0.8867	2.1638	0.2765	0.6416	0.8150	2.4798	0.3470	3.1479
4	0.7522	2.3835	0.5167	0.6931	0.2745	2.4004	0.6434	3.1396
5	0.5601	2.5369	0.6502	0.0584	0.8253	1.7670	0.5460	3.5519
6	0.5805	1.9447	0.8125	0.2457	0.8163	2.2921	0.7830	3.3528
7	0.4053	2.1997	0.7888	0.5849	0.7237	1.9326	0.5278	3.5762
8	0.4800	1.4588	0.9983	0.2215	0.7424	2.3059	0.3897	3.0723
9	0.6765	1.9546	0.9562	0.5801	0.3005	2.2163	0.6713	3.1016
10	0.1583	0.3216	0.4995	0.9880	0.4467	1.3062	0.5749	2.9375
11	0.5637	0.9158	0.7059	0.0427	0.5515	1.3406	0.5144	2.7375
12	0.4754	1.1517	0.6895	0.1591	0.5141	1.7258	0.7552	2.9168
13	0.5927	1.1166	0.6343	0.7283	0.2195	1.7107	0.7955	3.5109
14	0.4172	1.9780	0.5341	1.1535	0.2466	1.4386	0.3155	4.3239

The obtained results indicated that Table 3 portrays the comparison of side lobes level (SLL) and convergence speed (CS) performances of 12 elements 1-D array obtained by GSO and APSO. Accordingly, the genetical swarm optimizer algorithm achieved the best maximum side lobes level, and it converged more rapidly than the adaptive particle swarm optimization methodology in all the cases that have been dealt with.

Table 3. Comparison of SLL and CS performances of the 1-D arrays obtained by GSO and APSO

	Figure 5				**Figure 7**			
	TM_{11}		**TM_{12}**		**TM_{11}**		**TM_{12}**	
	SLL (dB)	**CS (cycles)**	**SLL (dB)**	**CS (cycles)**	**SLL (dB)**	**CS (cycles)**	**SLL (dB)**	**CS (cycles)**
APSO	-30	86	-30	23	-25	81	-30	57
GSO	-32	64	-35	19	-27.49	60	-33.50	46

5. CONCLUSION

This paper builds on a comparative study involving the adaptive particle swarm optimizer and the genetical swarm optimizer approaches with the aim to provide a synthesis of linear annular ring antenna arrays for the two modes TM_{11} and $TM_{12,}$ respectively. The hybrid algorithm was applied to improve the reduction of the side lobes level and convergence velocity. Comparison of the GSO and APSO for the selected set of examples revealed an improvement of paramount importance in terms of the side lobes level lowering and the number of iteration cycles diminution.

6. REFERENCES

[1] Chaker H, Null Steering and Multi-beams Design by Complex Weight of antennas Array with the use of APSO-GA. Wseas Trans Commun., 2014, 13(2):99–108

[2] Wang W B, Feng Q.Y, and Liu D. Synthesis of Thinned Linear and Planar Antenna Arrays using Binary PSO Algorithm. PR Electromagn Res., 2012, 127(1):371-387, https://doi.org/10.2528/PIER12020301

[3] Chaker H, Genetical Swarm Optimizer for Synthesis of Multibeam Linear Antenna Arrays. PR Electromagn Res C., 2015, 60 (1), 137-146, https://doi.org/10.2528/PIERC15110206

[4] Chatterjee S, Synthesis of linear array using Taylor distribution and Particle Swarm Optimization, Int. J. Elect., 2015, 102(3), 514–528, https://doi.org/10.1080/00207217.2014.905993

[5] CHAKER H, Abri M, and Badaoui H. Hybrid Evolutionary Algorithm Genetical Swarm Optimization for 1-D and 2-D Annular Ring Unequally Spaced Antennas Arrays Synthesis, Electromagnetics., 2016, 36(8), 1–19, https://doi.org/10.1080/02726343.2016.1236008

[6] Grimaccial F, Mussettal M, Pirinoli P, and Zichl R. E, Genetical Swarm Optimization (GSO): a class of Population-based Algorithms for Antenna Design, IEEE Int Conf Comm Elect, 2006, 467-471, https://doi.org/10.1109/CCE.2006.350871

[7] CHAKER H, Abri M, and Badaoui H. Multi-beam Ring Antenna Arrays Synthesis by The Application of Adaptive Particle Swarm Optimization, PR Electromagn Res M., 2016, 50(1), 169–181, https://doi.org/10.2528/PIERM16062202

[8] Chew W C, A Broad-Band Annular-Ring Microstrip Antenna, IEEE T Antenn Propag., 1982, 30(5), 918–922

[9] David M, Rigorous Analysis of Probe-Fed Printed Annular Ring Antennas, IEEE T Antenn Propag., 1999, 47(2), 384–388. https://doi.org/10.1109/8.761079

[10] Bhartia P. Bahl I, Garg R. Ittipiboon A. (2nd ed.) Microstrip Antenna Design Handbook. Artech House Antennas and Propagation Library, 2000.

[11] Abri M. Boukli-hacene N and Bendimerad F.T. Synthesis of ring printed antennas arrays: Optimization by the genetic algorithm, Int J Model Simul., 2008, 28(2), 174–181

[12] Ibarra M. Panduro M A, and Andrade A G. Differential Evolution Multi-Objective for Optimization of Isoflux Antenna Arrays. IETE Tech Rev., 2016, 33(2), 105-114. https://doi.org/10.1080/02564602.2015.1049222

[13] Panduro M A, Brizuela C A. Evolutionary multi-objective design of non-uniform circular phased arrays, Int J Comput Math elec Electron Eng., 2008, 27(2), 551 – 566.

[14] Owen P, Mason J.C. the use of linear programming in the design of antenna patterns with prescribed nulls and other constraints, INT J Comput Math elec Electron Eng., 1984, 3(4), 201 – 215.

[15] Deng H, Li X, Sun L, Yang S. Minimizing sidelobe levels and facilitating null placements of nonlinear antenna arrays using an improved particle swarm optimization method, INT J Comput Math elec Electron Eng., 2013, 33(1/2), 65-73.

https://doi.org/10.1108/COMPEL-11-2012-0334

[16] He G. Wu B. Unified particle swarm optimization with random ternary variables and its application to antenna array synthesis, J Electromagnet Wave., 2014, 28(6). 752-764, https://doi.org/10.1080/09205071.2014.888959

[17] Djennas S A. Benadda B. Merad L, and Bendimerad F T. Conformal antennas arrays radiation synthesis using immunity tactic, INT J Comput Math elec Electron Eng., 2014, 33(3), 1017-1037.

[18] Tej R. Kavya K.C.S, & Kotamraju S.K. Synthesis of phased array antenna for side lobe level reduction using the differential evolution algorithm. Int J Speech Technol., 2020, 23, 337–342. https://doi.org/10.1007/s10772-020-09701-2

[19] Abri M. Boukli-hacene N and Bendimerad F T. Ring Printed Antennas Arrays Radiation Application to Multibeam, presented at the Mediterranean Microwave Symposium, Marseille, France, June. 1-3, 2004.

[20] Abri M. Application du recuit simulé à la synthèse d'antennes en réseau constituées d'éléments annulaires imprimés, Ann Telecommun., 2005, 60(11), 1422–1438.

[21] XF Xie. WJ Zhang, and ZL Yang. Adaptive Particle Swarm Optimization on Individual Level, IEEE IC Digit Sig Proc., 2002, 1215-1218.
https://doi.org/10.1109/ICOSP.2002.1180009

[22] Kennedy J. The particle swarm: social adaptation of knowledge. IEEE IC Evol Computat., 1997, 303-308 https://doi.org/10.1109/ICEC.1997.592326

[23] Eberhart R. Shi Y. Particle swarm optimization: developments, applications and resources. IEEE IC Evol Computat., 2001, 81-86,
https://doi.org/10.1109/CEC.2001.934374

[24] Villegas F J. Parallel Genetic-Algorithm Optimization of Shaped Beam Coverage Areas Using Planar 2-D Phased Arrays. IEEE T Antenn Propag., 2007, 55(6), 1745-1753, https://doi.org/10.1109/TAP.2007.898601

[25] Chaker H. Badaoui H. Abri M, and Benadla I. Efficient synthesis of dual band selective filters using evolutionary methods in a 1D photonic crystal slab for near infrared applications. J Comput Electron., 2020, 19(1), 1-6, https://doi.org/10.1007/s10825-019-01439-8